

Experimental Demonstration of Learned Time-Domain Digital Back-Propagation

Eric Sillekens, Wenting Yi, Daniel Semrau, Alessandro Ottino, Boris Karanov, Sujie Zhou, Kevin Law, Jack Chen, Domani Lavery, Lidia Galdino, Polina Bayvel, and Robert I. Killey

Abstract—We present the first experimental demonstration of learned time-domain digital back-propagation (DBP), in 64-GBd dual-polarization 64-QAM signal transmission over 1014 km. Performance gains were comparable to those obtained with conventional, higher complexity, frequency-domain DBP.

I. INTRODUCTION

The non-linear fibre channel has a limited capacity due to increasing nonlinear signal distortions with increasing transmission power, leading to a peak in achievable information rate (AIR) for a fixed bandwidth. One approach to increase this maximum AIR is to mitigate the non-linear distortion. This can be achieved with digital signal processing (DSP) by solving the differential equation that describes the non-linear fibre response backwards, using the received signal as the initial condition. This method, known as split-step Fourier method (SSFM) based digital back-propagation (DBP) [1], has been shown to allow increased data throughput and transmission reach [2].

A significant drawback of the DBP technique is its computational complexity, making it challenging to implement in real-time systems. In conventional frequency-domain DBP (FD-DBP), dispersion compensation is performed in the frequency domain and nonlinear phase shifts are corrected in the time domain, requiring repeated conversions of the signal between the time and frequency domains using fast Fourier transforms. This leads to high computational complexity, particularly when small step-sizes, and hence a large number of steps, are used to achieve high accuracy. To reduce complexity, both dispersion and nonlinearity could be compensated in the time-domain (TD-DBP), with the dispersion compensation being carried out with tap-and-delay finite impulse response (FIR) filters [3]. However, low-order FIR filters are fundamentally unable to accurately compensate small amounts of dispersion. An approach to overcome this drawback was proposed in [4], [5], and involves applying machine-learning techniques to optimize the combined response of all the cascaded filters. The approach leverages the similarities between time-domain DBP and deep feed-forward neural networks; in both structures, linear filters and nonlinear functions are interleaved. The

recent rapid advances in algorithms, and readily available software packages, allow implementation of these algorithms for the optical transmission channel.

In this work, we experimentally demonstrate, for the first time, learned time-domain digital back-propagation. First, the method of training the required time-domain filter weights is explained. Next, the performance of the learned TD-DBP is assessed for 4-channel 64 GBd polarisation division multiplexing (PDM)-64QAM transmission over 1014 km, and compared with the performance of conventional frequency-domain DBP. Finally, the resulting filter tap weights and frequency response of the FIR filters are analysed. We observed performance improvements over linear compensation comparable to those obtained using the conventional FD-DBP implementation.

II. DIGITAL BACK-PROPAGATION

DBP implements the non-linear Schrödinger equation (NLSE) for each step in two parts. For a step starting at distance z along the fibre, firstly, the chromatic dispersion and loss are applied, in the frequency domain (in the case of the conventional FD-DBP implementation) as a linear operator, and the non-linear phase shift is performed in the time domain, using the respective transformations;

$$E(\omega, z + \Delta z) = e^{\alpha \Delta z} e^{jK(\omega T)^2} E(\omega, z) \quad (1)$$

$$E(t, z + \Delta z) = e^{-j\gamma \Delta z |E_z(t)|^2} E(t, z), \quad (2)$$

where α is fibre loss, Δz is fibre step length, $K = \frac{\beta_2 \Delta z}{2T^2}$, ω angular frequency, T sampling period, and β_2 group velocity dispersion, γ the nonlinearity coefficient and $|E_z(t)|^2$ the normalised, step-averaged, instantaneous optical power.

In the time-domain DBP approach, the chromatic dispersion part of each step is applied using a time-domain finite impulse response (FIR) filter (tap-and-delay filter). The full-band least-squares FIR filter design from [6] could be used with a total number of taps given by $N_c \leq 2\lfloor 2\pi K \rfloor + 1$. However, as described in [4], if the filter tap weights given by [6, Eq. (13)] are used for the multiple cascaded low-order FIR filters in the DBP, the ripples introduced into the frequency response result in large performance penalties, negating the gains achieved through the non-linearity mitigation. The solution proposed in [4] is to update all the FIR filter weights simultaneously using algorithms which have been developed to update the weights in deep feed-forward neural networks. The method consists of implementing the dispersion as a convolutional layer and the fibre phase shift as a non-linear activation function.

Eric Sillekens, Wenting Yi, Daniel Semrau, Alessandro Ottino, Boris Karanov, Domani Lavery, Lidia Galdino, Polina Bayvel, and Robert I. Killey are with the Optical Networks Group, Dept. Electronic & Electrical Engineering, UCL, London WC1E 7JE, U.K.

Sujie Zhou and Jack Chen are with Huawei Chengdu Research Institute U1, Chengdu, Sichuan Province, P.R. China, Postal Code 611731

Kevin Law is with Huawei Base G6, Dongguan, Guangdong Province, P.R. China, Postal Code 523808

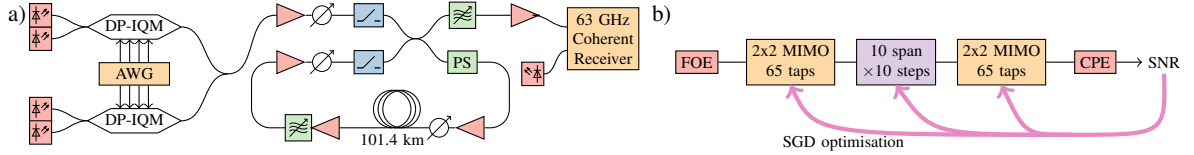


Fig. 1. a) Experimental configuration with 4×30 GBd channels and 101.4 km recirculating loop. Function diagram of the receiver DSP for the L-TDDBP (b).

In this work, the deep learning of the filter weights (equivalent to a neural network's layer parameters) is implemented in Tensorflow using the RAdam optimiser [7]. Identical complex FIR filter weights are applied to both polarisations in each step, reducing the overall number of weights to be optimized. Initialisation of the time-domain filter taps was carried out via numerical simulation of the fibre transmission link for a single channel. The forward propagation was modelled using a small NLSE fibre step size (100 m) at a launch power of 5 dBm (beyond optimum launch power for linear compensation). Starting from the least squares solution [6], a set of 10 filters was designed using a 10 span simulation. Note, these filters purely compensate fibre transmission and no transceiver impairments. Further training of the filters was carried on the experimental waveforms, before the performance was tested.

III. EXPERIMENTAL SETUP

The experimental setup is shown in Fig. 1(a). A fibre transmission distance of 1014 km was emulated using a recirculating loop. The waveform of the 64-QAM 64-GBd channel under test (CUT) was generated offline and sent to two channels of a 33-GHz 92-GSa/s arbitrary waveform generator (AWG) and, using a dual-polarization IQ modulator (IQM), modulated the outputs of two <100 kHz external cavity lasers (ECLs). Two additional 64-QAM 64-GBd aggressor channels were modulated using an additional AWG with a dual polarization IQM onto two ECLs and interleaved with the other channels to achieve uncorrelated sequences between neighbouring WDM channels. The recirculating loop with a 101.4 km span, a polarisation scrambler (PS) and three Erbium doped fibre amplifiers (EDFA) and an optical band-pass filter had the signal circulating 10 times, totalling a 1014 km transmission. At the receiver an optical band pass filter followed by an EDFA extracts the CUT for detection with a coherent receiver employing 63-GHz bandwidth 160-GS/s analogue-to-digital converters.

For this experimental demonstration, 10 steps per span were chosen for the learned TD-DBP. To take fibre loss into account, non-uniform FIR filter lengths were employed, implementing steps with equal power differences between their inputs and outputs. For the fibre nonlinearity compensation of 10 spans of 101.4 km each, the parameters were α of 0.16 dB/km, β_2 of -20.18 ps²/km and γ_{DBP} of 0.8 1/W/km. The 10 FIR filters used in the TD-DBP employed a total of 270 complex-valued tap weights at a sampling rate of 128 GSa/s. For the FD-DBP, 50 equidistant steps/span were used. This requires $2 \times 10 \times 50$ FFT operations per polarisation, while in the TD-DBP scheme the use of FFT operations is circumvented, lowering the computational complexity.

Next, for the processing of experimental data, the filter weights from simulation were used for initialisation. To prevent the dispersion filters from learning the response of the transceiver impairments, an additional 2x2 multiple input, multiple output (MIMO) filter was added before applying digital back propagation, as shown in Fig. 1(b). Thus, the resulting structure has two linear MIMO equalisers, compensating for PMD and transmitter and receiver impairments. Note that in this way, using the automatic differentiation in Tensorflow, the filter that is applied prior the link compensation is also optimized through gradient descent. A root-raised cosine (RRC) filter was applied before the MIMO blocks. The carrier phase estimation was achieved by inserting pilot symbols. One in 32 symbol was a known quadrature phase shift keyed symbol (QPSK). Interpolation of the phase between the pilot symbols was performed using a Wiener filter [8, Eq. (32)], following which a mean-squared-error cost is calculated.

During the training procedure, first the linear filters at both sides of the link compensation were optimized. Subsequently, all filters were updated on each optimisation step. For the FD-DBP, the α , γ and launched power were swept for optimisation, after which pilot-aided DSP was applied. For the experimental waveform, a single randomly generated 2^{16} -symbol waveform was used. We split the bit sequence and corresponding received waveforms into two datasets. The first 5224 symbols (80%) were used as training data for updating the filter weights. The remaining 13312 symbols (20%) were used as testing data, to obtain results reported in the figures presented.

IV. RESULTS

The launched power was increased with 1 dB increments from -6 to +8 dBm per channel. The resulting SNR, defined as $\frac{E[|X|^2]}{E[|X-Y|^2]}$, where X and Y are the transmitted and received signal respectively. Fig. 2(a) shows a comparison of achieved SNR for TD-DBP, FD-DBP and EDC. The TD-DBP and FD-DBP are implemented using 10 and 50 steps per span respectively. Both schemes provide similar performance improvements from non-linearity compensation, with slightly higher accuracy in the high power regime for the conventional FD-DBP scheme, due to the larger number of steps used. However, the TD-DBP achieves a higher SNR in the low power regime, suggesting a better linear compensation. Fig. 2(b) compares TD-DBP with two learned linear compensation strategies. The figure shows the learned DBP performance for two cases, the proposed non-linear mitigation scheme, and the same scheme with $\gamma_{\text{DBP}} = 0$, i.e., providing only linear compensation and a scheme where the whole chromatic dispersion is compensated

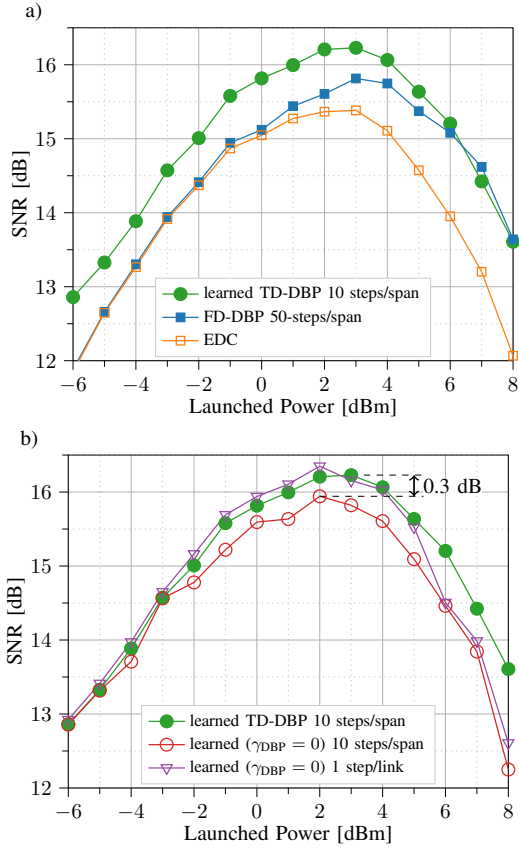


Fig. 2. a) SNR vs. launched power for learned TD-DBP compared to conventional FD-DBP and linear EDC only methods. b) TD-DBP compared to the same structure with $\gamma_{DBP} = 0$ with the same number of steps and a single step for the whole link.

in a single filter. For a low launched power into the fibre, the first two schemes show comparable performance, while a non-linearity mitigation gain of 0.3 dB is achieved at optimal launch powers. Using a single filter achieves better linear gain, but converges to the $\gamma_{DBP} = 0$ method in the high launched power regime.

To confirm that the algorithm is performing digital back-propagation, i.e., approximating the SSFM model, the amplitude response and group delay of the 10 individual filter used each span are plotted in Fig. 3. The expected response is an all-pass filter (H) with a linear group delay ($\Delta\tau$), compensation for chromatic dispersion. It can be seen that, while the individual filters have significant ripples, the combined filter, depicted as the last subplot of Fig. 3, has an almost perfect response within the signal bandwidth, with a flat amplitude response and a smooth group delay.

V. FUTURE WORK

We have also trained a single convolutional layer for the whole link to apply the chromatic dispersion compensation and shown the results in Fig. 2. This method outperforms all other methods up until optimal launched power. However for high launched powers the performance converge to the linear compensation results. When looking at the auto-correlation of the single learned filter in Fig. 4, we can see bumps where

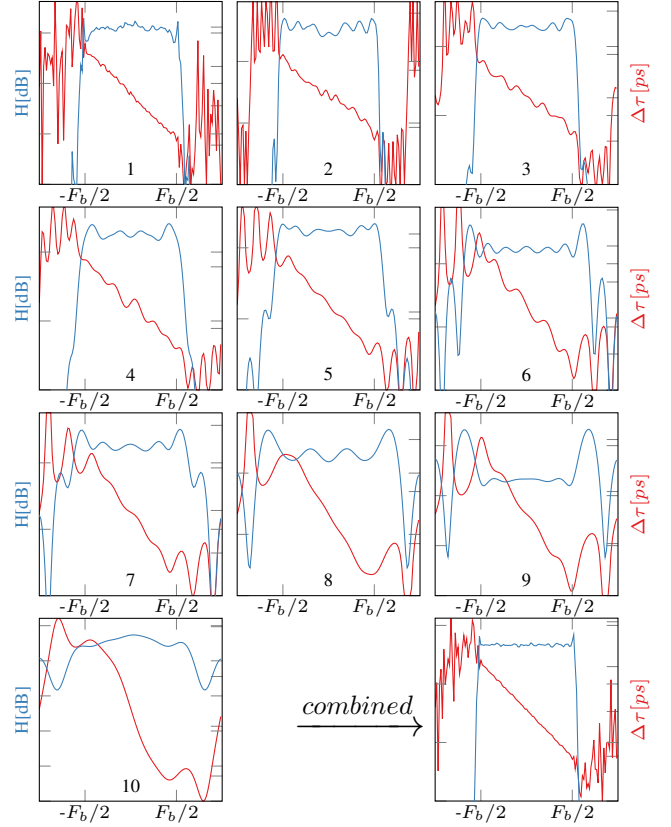


Fig. 3. Amplitude response and group delay of the 10 individual filters used every span. Bottom right: combined response of all 10 cascaded filters.

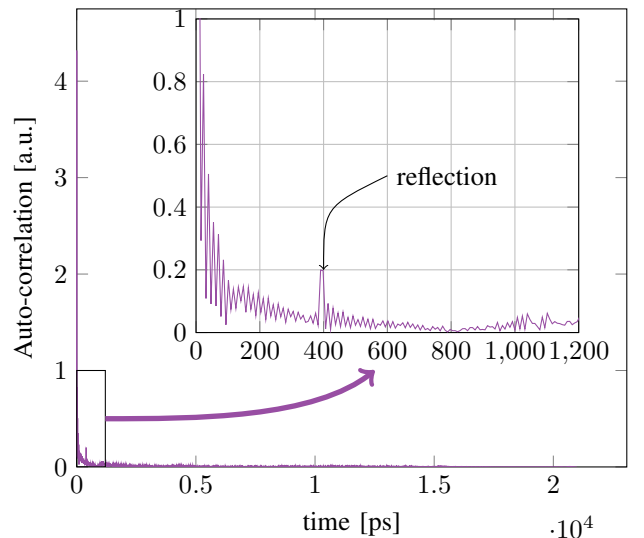


Fig. 4. The auto-correlation of the learned single filter used to compensate chromatic dispersion.

the filter has compensated a reflection. This suggests that not all the linear effects are compensated for and combining this result with nonlinear compensation will increase the performance even further.

We suspect the difference in performance between the single layer and the deep network to partially be attributable to gradient propagation through the many layers, in this work over 100. A method to combat this is proposed in [9], where residual links are bypassing the layer. The result are equivalent due to the universal function approximates used. When trying to learn $x_{k+1} = \mathcal{U}\{x_k\}$ will be equivalent to learning $x_{k+1} = x_k + \mathcal{V}\{x_k\}$ if $\mathcal{V}\{x\} \triangleq \mathcal{U}\{x\} - x$. These layers have the gradient

$$\frac{\partial x_{k+1}}{\partial x_k} = \mathcal{U}'\{x_k\} \quad (3)$$

$$\frac{\partial x_{k+1}}{\partial x_k} = 1 + \mathcal{V}'\{x_k\} \quad (4)$$

but if two layers are applied sequentially, the gradient becomes

$$x_{k+2} = \mathcal{U}\{\mathcal{U}\{x_k\}\} \quad (5)$$

$$\frac{\partial x_{k+2}}{\partial x_k} = \mathcal{U}'\{x_{k+1}\}\mathcal{U}'\{x_k\} \quad (6)$$

$$\frac{\partial x_{k+2}}{\partial x_k} = 1 + \mathcal{V}'\{x_{k+1}\}(1 + \mathcal{V}'\{x_k\}) \quad (7)$$

We can see the direct function will have a multiplicative term for every layer, but the residual link will propagate the constant through all the layers and therefore a more direct link with the error function.

For the DPB we can see this calculation the chromatic dispersion and nonlinear phase shift as perturbation to our signal. This is a different approach then the perturbation DBP [10], [11], although it shares some thoughts.

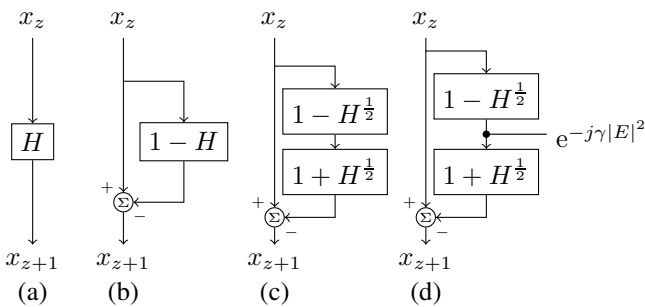


Fig. 5. The proposed digital back-propagation block. (a) a single dispersion block (b) add the residual link (c) split the block into to half steps (d) add the nonlinear phase shift.

In Fig. 5, the proposed block with the residual link is shown (d). The block is designed from starting with a dispersion block in the frequency domain $x_{k+1} = H(x) = xe^{-jK(\omega T)^2}$, which can either be applied directly (a) or with a residual link (b). However, in (c) we have split the dispersion step such that

we have

$$\begin{aligned} x_{k+1} &= x_k - x_k \left(1 - e^{-\frac{jK(\omega T)^2}{2}}\right) \left(1 + e^{-\frac{jK(\omega T)^2}{2}}\right) \\ &= x_k - x_k \left(1 - \left(e^{-\frac{jK(\omega T)^2}{2}}\right)^2\right) \\ &= x_k e^{-jK(\omega T)^2} \end{aligned} \quad (8)$$

Now we have split the step, we can apply the nonlinear phase shift in the middle of the block. Effectively recreating a split step method with a residual link.

VI. CONCLUSION

We experimentally demonstrated learned time-domain digital back-propagation for the first time. The learned algorithm was verified to approximate the NLSE model, showing flat amplitude response and smooth group delay for the cascaded filters. Overall, an SNR improvement due to non-linearity mitigation of 0.3 dB was achieved, comparable with conventional mitigation algorithms.

Financial support by EPSRC TRANSNET and EU COIN. E. Sillekens funded by EPSRC grant EP/M507970/1.

REFERENCES

- [1] E. Ip and J. M. Kahn, "Compensation of dispersion and nonlinear impairments using digital backpropagation," *J. Lightw. Technol.*, vol. 26, no. 20, pp. 3416–3425, Oct 2008.
- [2] L. Galdino *et al.*, "On the limits of digital back-propagation in the presence of transceiver noise," *Opt. Express*, vol. 25, no. 4, pp. 4564–4578, Feb 2017.
- [3] C. Fougstedt *et al.*, "Time-domain digital back propagation: Algorithm and finite-precision implementation aspects," in *OFC*, 2017, p. W1G.4.
- [4] C. Häger and H. D. Pfister, "Nonlinear interference mitigation via deep neural networks," in *OFC*, 2018, p. W3A.4.
- [5] —, "Deep learning of the nonlinear schrödinger equation in fiber-optic communications," in *IEEE ISIT*, Jun. 2018, pp. 1590–1594.
- [6] A. Eghbali *et al.*, "Optimal least-squares fir digital filters for compensation of chromatic dispersion in digital coherent optical receivers," *J. Lightwave Technol.*, vol. 32, no. 8, pp. 1449–1456, Apr 2014.
- [7] J. M. Kblera *et al.*, "An adaptive optimizer for measurement-frugal variational algorithms," 2019, arXiv:1909.09083.
- [8] E. Ip and J. M. Kahn, "Feedforward carrier recovery for coherent optical communications," *J. Lightw. Technol.*, vol. 25, no. 9, pp. 2675–2692, Sep 2007.
- [9] K. He, X. Zhang, S. Ren, and J. Sun, "Deep residual learning for image recognition," 2015, arXiv:1512.03385.
- [10] X. Liang and S. Kumar, "Multi-stage perturbation theory for compensating intra-channel nonlinear impairments in fiber-optic links," *Opt. Express*, vol. 22, no. 24, pp. 29 733–29 745, Dec 2014.
- [11] W. Yan, Z. Tao, L. Dou, L. Li, S. Oda, T. Tanimura, T. Hoshida, and J. C. Rasmussen, "Low complexity digital perturbation back-propagation," in *ECOC*, Sep. 2011, p. Tu.3.A.2.